Sains Malaysiana 46(11)(2017): 2019-2028
http://dx.doi.org/10.17576/jsm-2017-4611-01

Study on the Characteristics of Gas Permeability of Coal under Loaded Stress
(Kajian Pencirian Kebolehtelapan Gas Arang Batu di bawah Beban Tekanan)

Dengxing Qu, Xinping Li, Jianhua Zhang*, Dengke Li & Gongzhong Wang

ABSTRACT

The #3 coal seam of Jinsheng Rundong Ltd. of Jin-Coal Group in Shanxi Province, China, has high gas content and pressure; however, it has a low gas permeability, which can easily cause gas enrichment and may cause accidents of coal and gas outbursts. In this work, the characteristics of gas seepage were thoroughly studied by designing and modifying the 'complete stress-strain tri-axial servo temperature-controlled test system'. The study was conducted based on four factors: Axial pressure, confining pressure, effective stress and gas pressure. We found that the axial pressure has a weak impact on coal gas permeability, indicated by a linear relationship. The confining pressure, however, has a strong impact on gas permeability, showing an exponential relationship. The relationship between permeability and gas pressure was identified as a second-order polynomial function. The functional relationship between gas permeability and axial pressure, confining pressure, effective stress, gas pressure was analyzed. Investigation into the natural flow rate of gas, concentration of gas drainage and damping coefficient supported the conclusion from the experimental study on the characteristics of gas seepage under loaded stress.

Keywords: Field test; gas within coal; load stress; permeability

ABSTRAK

Lipit arang batu #3 daripada Jinsheng Rundong Ltd. diperoleh daripada Kumpulan Jin-Coal di Wilayah Shanxi, China mempunyai kandungan dan tekanan gas yang tinggi; walau bagaimanapun, ia mempunyai kebolehtelapan gas yang rendah dan dengan mudah boleh menyebabkan pengayaan gas yang boleh menyebabkan kemalangan arang batu dan letusan gas. Dalam kajian ini, ciri resapan gas telah dikaji secara teliti dengan merancang dan mengubah suai 'sistem pengujian suhu-terkawal servo tri-paksi tekanan yang lengkap'. Kajian ini dijalankan berdasarkan empat faktor: Tekanan paksi, tekanan mengekang, tegasan berkesan, dan tekanan gas. Kami mendapati bahawa tekanan paksi mempunyai kesan lemah terhadap ketelapan gas arang batu, seperti ditunjukkan pada hubungan lurus. Walau bagaimanapun, tekanan pengurung mempunyai kesan yang besar terhadap kebolehtelapan gas, yang menunjukkan hubungan eksponen. Hubungan antara kebolehtelapan dan tekanan gas dikenal pasti sebagai fungsi polinomial-tertib kedua. Hubungan fungsi antara kebolehtelapan gas dan tekanan paksi, tekanan mengekang, tegasan berkesan dan tekanan gas dianalisis. Kajian kepada kadar aliran gas semula jadi, kepekatan saliran gas dan pekali redaman menyokong kesimpulan daripada kajian eksperimen mengenai ciri resapan gas di bawah beban tekanan.

Kata kunci: Beban tekanan; gas dalam arang batu; kebolehtelapan; ujian lapangan

Introduction

The #3 coal seam of Jinsheng Rundong (JSRD) Ltd. of the Jin Coal Group in Shanxi Province, China, has a high gas content and pressure; however, it has a low permeability, which can easily cause the enrichment of gas and may cause accidents of coal and gas outbursts.

The gas seepage theory is currently the main theory to guide the prevention of gas accidents in coal mines. Some of researcher also investigated the change in permeability of methane gas through a coal sample using the true tri-axial stress permeameter (Palmer 2008; Wang et al. 2008). Besides, some scientist established the model of methane flow in the coalbed, and analyzed the outbursts of coal and gas (Fathi & Akkutlu 2009; Fedorov & Fedorchenko 2009). Furthermore, some paper research also focused on gas transportation in the coal bed (Han et al. 2009; Pan et al. 2010). A research conducted the study on the permeability change of coal during the rupture process, based on successful coal sampling using the 'twice moulding' method (Kunyun 2014). On the basis of damage mechanics, rock mechanics, and osmotic mechanics, combined experiments and theoretical study, and obtained the relationship between coalbed permeability and different factors such as tri-confining stress, gas pressure in the coalbed, and periodical excavation perturbation (Bobo 2014; Mingyao 2013). A researcher analyzed the evolution mechanism of cracks using a dynamic method based on the complete stress-strain permeability test and the observation of the property changes in the crack structure (Wang et al. 2012).

During the production practice in the #3 coal seam of JSRD Ltd., the coal seams located within the stress-concentrated zone generally have a higher gas pressure than those located outside of the stress-concentrated zone (Lai et al. 2017). The stress-concentrated zone has low gas permeability, with a higher tendency for gas enrichment. In addition, drastic stress change occurs between the stress-concentrated and stress-diluted zone, which can cause coal and gas outbursts. At present, many gas management methods used to treat coal seams with low permeability are based on the mechanism of pressure-relief and permeability-enhancement, such as hydraulic cracking, hydraulic drilling of holes, and high-pressure water jets. The purpose of these methods is to transform the stress-concentrated zone into a stress-diluted zone, and increase the permeability of the coal seam to reduce the risk of outbursts. Therefore, analysis of the impact of the stress field change on the permeability of coal seams is crucial to prevent gas accidents in coal mines.

Materials and Methods

COAL SAMPLING

In this work, coal samples were collected from the #3 coal seam of JSRD Ltd. The Protodikonov's hardness coefficient of the samples is around 1. Coal sampling was conducted at the 1301 fully mechanized coal face at 250 m depth. Collected samples were manufactured to have 2:1 height/diameter, i.e., the diameter (Φ) and length (*l*) of the cylindrical coal samples were 50 mm and 100 mm, respectively.

EXPERIMENTAL DEVICES AND DESIGN

The self-designed and modified 'complete stress-strain tri-axial servo temperature-controlled test system' is composed of a coal sealing system, axial and confining pressure load system, automatic temperature control system, automatic negative pressure control system, and the data monitoring and acquisition system for flow, stress, and strain.

Previous research unanimously indicates that there are many factors that can affect the gas permeability of coal seams, such as stress, gas pressure, negative pressure for draining, and temperature (Mavor & Gunter 2006; Peng et al. 2008; Sun & Ling 2000). Therefore, in order to fully understand the permeability of a coal seam, experiments must be conducted under different gas pressures, negative pressures for draining, and effective stresses (Kamsani et al. 2017). The effective stress in this work refers to the average effective stress (Yi et al. 2007), i.e.

$$\sigma_{\epsilon} = (\sigma_1 + 2\sigma_2) / 3 - (P_1 - P_2) / 2 \quad , \qquad (1)$$

where, σ_1 is the axial pressure (MPa); σ_2 is the confining pressure (MPa); and P_1 and P_2 are the inlet and outlet gas pressure of the sample (MPa), respectively. The average effective stress σ_{ϵ} is referred to as the 'effective stress' throughout this paper.

To study the effect of stress in the coal seam on gas permeability, the experimental temperature was controlled at a constant 25°C. Axial and confining pressure were set at 1.0, 2.0, 3.0, 4.0, 5.0, 6.0, 7.0, 8.0, 9.0 and 10.0 MPa; and the gas pressure at the inlet was controlled at 0.5, 0.8, 1.0, 1.2 and 1.5 MPa. The detailed parameters of the experimental design are shown in Tables 1, 2 and 3, and were adopted for three different coal samples.

TABLE 1. Experimental design for studying the effects of axial and confining pressure on gas permeability of coal samples

Group	Gas pressure (MPa)	Negative pressure for draining (kPa)	Axial pressure (MPa)	Confining pressure (MPa)
I-1–I-10	1.0	15.0	1.0–10.0	2.0
I-11–I-20			1.0–10.0	4.0
I-21–I-30			1.0–10.0	6.0
I-31–I-40			1.0–10.0	8.0
I-41–I-50			1.0–10.0	10.0
I-51–I-60			2.0	1.0–10.0
I-61–I-70			4.0	1.0–10.0
I-71–I-80			6.0	1.0–10.0
I-81–I-90			8.0	1.0–10.0
I-91–I-100			10.0	1.0–10.0

TABLE 2. Experimental design for studying the effects of effective stress on gas permeability

Group	Gas pressure (MPa)	Negative pressure for draining (kPa)	Effective stress (MPa)	Confining pressure (MPa)	Axial pressure (MPa)
II-1			1.0	1.75	1.0
II-2			2.0	2.75	2.0
II-3	1.0	15.0	3.0	3.75	3.0
II-4			4.0	4.75	4.0
II-5			5.0	5.75	5.0

TABLE 3. Experimental design for studying the effects of gas pressure on gas permeability

Group	Gas pressure (MPa)	Negative pressure for draining (KPa)	Axial pressure (MPa)	Confining pressure (MPa)
III-1	0.5, 0.8, 1.0, 1.2, 1.5		4.0	2.0
III-2	0.5, 0.8, 1.0, 1.2, 1.5	15.0	4.0	4.0
III-3	0.5, 0.8, 1.0, 1.2, 1.5		4.0	6.0
III-4	0.5, 0.8, 1.0, 1.2, 1.5		4.0	8.0

DATA ACQUISITION

Since the raw samples from the coal mine were used in this experiment, certain variation occurs from sample to sample. To avoid the extreme cases and produce a rigorous study of the impact of loaded stress on gas permeability, three coal samples were collected for each experimental group in this study, and the geometric average value was calculated, as shown below:

$$Q_\varepsilon=\sqrt[3]{\Pi_{i-1}^{3} Q_i}\ , \tag{2}$$

where Q_ε is the average flow rate of the three coal samples; and Q_i is the flow rate of each individual coal sample (i = 1, 2, 3).

ANALYSIS OF EXPERIMENTAL RESULTS

Following the aforementioned experimental design for the recording and processing of experimental data, we obtained the impact of axial pressure, confining pressure, and gas pressure on the gas permeability of coal sample. Factors such as coalbed pressure, coal rock patterns and cracks cause a large variation in the effects of axial pressure and confining pressure on the gas permeability of the coal sample (Kamsani et al. 2017). Thus, we discuss the individual impact of four aspects in this work: axial pressure, confining pressure, effective stress and gas pressure.

IMPACT OF AXIAL PRESSURE ON THE GAS PERMEABILITY OF THE COALBED

The collected flow rate is the average flow rate of methane gas in coal samples. Here Darcy's law was used to convert the flow rate into the more intuitive permeability parameter. The following equation was used in this work for the conversion:

$$K=\frac{Q^{'}\mu_g L}{A\left(P_1^2-P_2^2\right)}\ , \tag{3}$$

where A is the cross sectional area of the coal sample (cm^2); L is the height of the coal sample (cm); μ_g is the viscosity of methane gas (cp); P_1 and P_2 are the pressure of the two ends of the sample (atm); $\bar{Q}$ is the average gas flow rate; $\bar{Q}^{'}=\frac{2P_0Q_0}{P_1+P^2}$, (cm^3/s); and Q_0 is the gas flow rate under standard pressure (cm^3/s).

Our results showed that the tectonic coal seam has largest permeability in the direction parallel to the bedding. There was a large difference between the permeability in the direction parallel to the bedding and that vertical to the bedding. Tectonic coal has much larger gas permeability in the direction parallel to the bedding compared with that vertical to the bedding. In Experiments I-1 to I-50, axial pressure was considered as a single factor to investigate its impact on the gas permeability. Thus, constant confining pressure were set as follows: σ_2=σ_3=2MPa, σ_2=σ_3=4MPa, σ_2=σ_3=6MPa, σ_2=σ_3=8MPa, σ_2=σ_3=10MP . Axial pressure (σ_1) was chosen between 1–10 MPa.

The influence of temperature was excluded here, and the temperature was set to a constant 25°C. To better mimic the working conditions of the #3 coal seam of JSRD Ltd., gas inlet pressure was set to 1.0 MPa as the measured average gas pressure (P_1). Negative pressure of extraction was set as -15 kPa as the normal negative pressure for draining (Lai et al. 2017).

The data showing the effect of axial pressure on the permeability at confining pressures σ_2=σ_3= 2 MPa,σ_2=σ_3 = 4 MPa, σ_2=σ_3 = 6 MPa,σ_2=σ_3 = 8 MPa, and σ_2=σ_3= 10 MPa are shown in Figure 1.

Figure 1(a) - 1(e) shows the fit of permeability to confining pressure data at confining pressures σ_2 = 2, 4, 6, 8, and 10 MPa, respectively. These five sets of data indicate that the permeability is linearly related to axial pressure (σ_1) in the range of 1-10 MPa. Table 4 was obtained by linearly fitting the curve based on (4):

$$K=b+a\sigma_1, \tag{4}$$

where a and b are fitting coefficients.

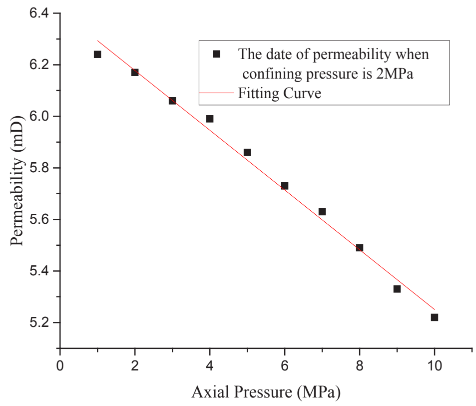

(a) Confining pressure = 2 MPa

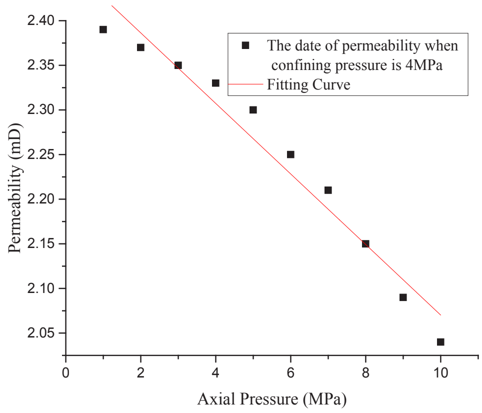

(b) Confining pressure = 4 MPa

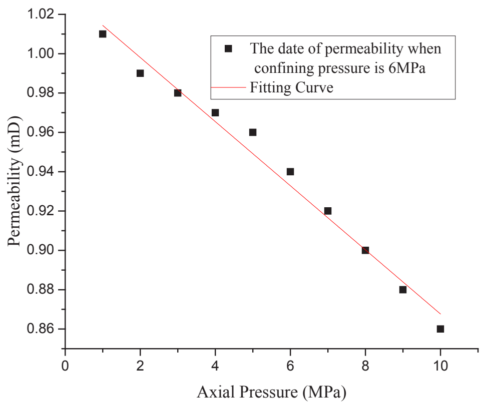

(c) Confining pressure = 6 MPa

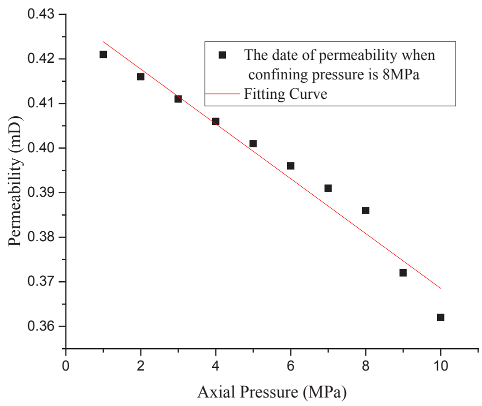

(d) Confining pressure = 8 MPa

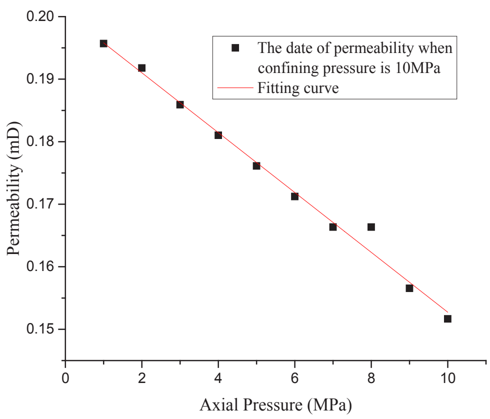

(e) Confining pressure = 10 MPa

FIGURE 1. Permeability versus axial pressure at 2–10 MPa confining pressure (σ_2)

TABLE 4. Fitted equation of permeability versus axial pressure at 2-10 MPa confining pressure

Group	Axial pressure (MPa)	Confining pressure (MPa)	Fitted equation	R^2
I-1–I-10	1–10	2	$K = 6.40933 - 0.11588\,\sigma_1$	0.99058
I-11–I-20	1–10	4	$K = 2.46223 - 0.03919\,\sigma_1$	0.94924
I-21–I-30	1–10	6	$K = 1.03255 - 0.01631\,\sigma_1$	0.98185
I-31–I-40	1–10	8	$K = 0.42988 - 0.00611\,\sigma_1$	0.95461
I-41–I-50	1–10	10	$K = 0.20059 - 0.00479\,\sigma_1$	0.98792

Table 4 shows that the equation $K=b+a\sigma_1$ has a good fit with the experimental data. Furthermore, the fitting coefficient *b* decreases with the increase of confining pressure, and the absolute value of *a* deceases with the increase of confining pressure. This indicates that with the increase of confining pressure, the effect of axial pressure on gas permeability decreases.

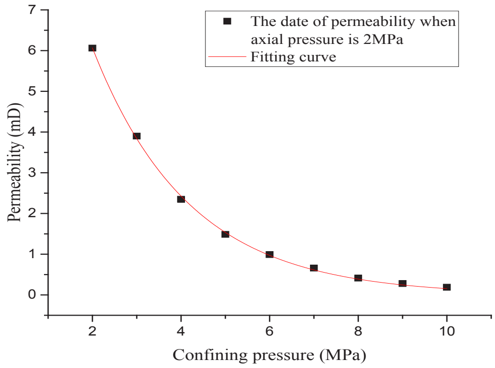

(a) Axial pressure = 2 MPa

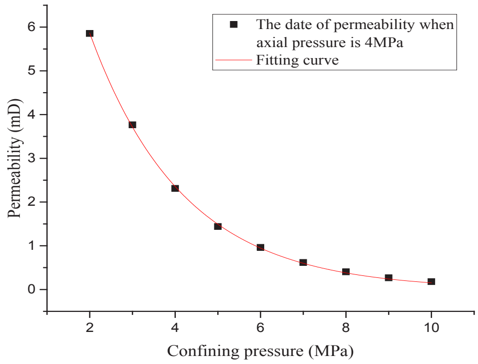

(b) Axial pressure = 4 MPa

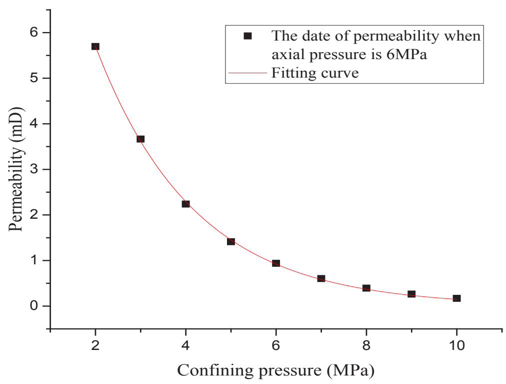

(c) Axial pressure = 6 MPa

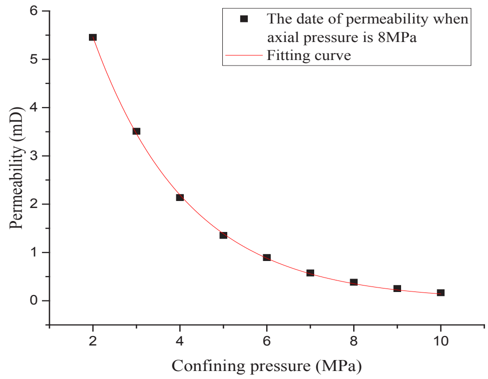

(d) Axial pressure = 8 MPa

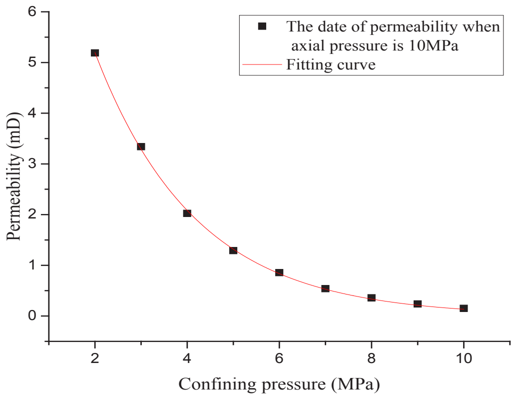

(e) Axial pressure = 10 MPa

FIGURE 2. Permeability versus confining pressure at 2–10 MPa axial pressure (σ_1)

Thus, for the coal samples collected from the #3 coal seam of JSRD Ltd., at the confining pressures (σ_2=σ_3) of 2, 4, 6, 8, and 10 MPa, the permeability of coal rock (K) can be regarded to follow the relationship described by Eq. 4 in the axial pressure (σ_1) range of 1–10 MPa. In (4), the linear slope ranges from -0.11588 to -0.00479, which indicates that the change of axial pressure has little impact on permeability under the normal axial pressure range (σ_1= 1-10 MPa).

THE IMPACT OF CONFINING PRESSURE ON THE PERMEABILITY OF THE COAL SAMPLE

In experiments I-51 to I-100, axial pressure was considered as a single factor to investigate its impact on the gas permeability (Kadir et al. 2013). Again, constant axial pressures were set as follows: σ_1= 2, 4, 6, 8 and 10 MPa. Confining pressure (σ_2=σ_3) was chosen between 1-10 MPa. Influence of temperature was excluded here, and the temperature was set constant at 25°C. To better mimic the working condition of the #3 coal seam of JSRD Ltd., gas inlet pressure (P_1) was chosen to be 1.0 MPa as the measured average gas pressure. Negative pressure for draining was chosen to be the normal extraction gas pressure, P_2= –15 kPa.

The experimental data are shown in Figure 2, which shows the impact of axial pressure on permeability at confining pressure σ_2=σ_3= 2 MPa, σ_2=σ_3= 4 MPa, σ_2=σ_3 = 6 MPa, σ_2=σ_3 = 8 MPa, and σ_2=σ_3 = 10 MPa.

Figure 2 shows that the nature of the permeability increase with confining pressure is different from that with axial pressure. The curve shows an approximately exponential function. The permeability of coal sample drastically decreases with confining pressure from 2 to 4 MPa; however, from 4 to 10 MPa confining pressure, the variance of permeability becomes smooth. This phenomenon occurs because with the gradual increase of confining pressure, the coal body undergoes shrinkage strain and the holes and cracks inside the coal body gradually close under compression, which reduces the permeability (Kadir et al. 2013). Previous research suggests that the impact of confining pressure on permeability of coal rock fits the exponential function in (5):

$$K=ae^{b\sigma_2}, \tag{5}$$

where a and b are fitting coefficients (Bobo 2014).

Thus, the curve of permeability against confining pressure was fit based on (5), giving the fitted equation describing permeability versus confining pressure under different axial pressures, as shown in Table 5.

TABLE 5. Fitted equation of permeability versus confining pressure based on experimental data at 2-10 MPa axial pressure

Group	Axial pressure (MPa)	Confining pressure (MPa)	Fitted equation	R^2
I-51–I-60	2	1–10	$K = 14.45417e^{-0.43478\sigma_2}$	0.99937
I-61–I-70	4	1–10	$K = 14.59494e^{-0.45601\sigma_2}$	0.99962
I-71–I-80	6	1–10	$K = 14.89240e^{-0.45578\sigma_2}$	0.99961
I-81–I-90	8	1–10	$K = 13.59622e^{-0.45616\sigma_2}$	0.99957
I-91–I-100	10	1–10	$K = 12.95996e^{-0.45696\sigma_2}$	0.99956

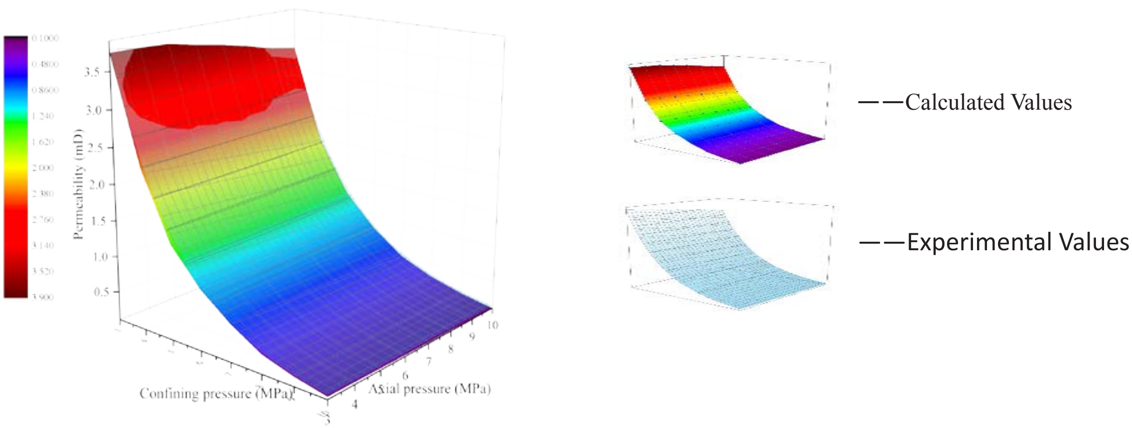

FIGURE 3. Comparison between experimental and calculated value of permeability at 2-10 MPa axial pressure and 2–10 MPa confining pressure

The R^2 for all samples were greater than 0.999, indicating very good fit of this model for permeability versus confining pressure. In addition, the fitting coefficient b in all the five fitting equations was close to -0.45. Thus, the fitting coefficient b of this coal rock can be determined to be -0.45. The fitting equation was determined as:

$$K=ae^{-0.45\sigma_2}, \tag{6}$$

where a is the fitting coefficient.

Figure 2(a) - 2(e) was fitted again based on (6), showing a good fit again with R^2 greater than 0.999. Moreover, it can be seen that the fitting coefficient a decrease with the increase of axial pressure. Therefore, under the aforementioned experimental conditions, the functional relationship between fitting coefficient a and confining pressure σ_1 was obtained as follows:

$$K=15.42623-0.26194\sigma_1 , \tag{7}$$

Substitute (7) into (6) gives:

$$K=15.42623e^{-0.45\sigma_2}-0.26194e^{-0.45\sigma_2} , \tag{8}$$

Figure 3 shows a comparison between experimental data with the data calculated by the fitted equation. As shown in Figure 3, under working conditions of gas pressure P_1 = 1.0 MPa and temperature T = 25°C, axial and confining pressure between 2-10 MPa, the experimental value has a good consistency with the value calculated using (8). Therefore, for the #3 coal seam of JSRD Ltd., under the condition of gas pressure P_1 = 1.0 MPa and temperature T = 25°C, axial and confining pressure between 2-10 MPa, permeability K of coal rock can be regarded to follow the relationship described by (8).

IMPACT OF EFFECTIVE STRESS ON THE GAS PERMEABILITY OF THE COAL SAMPLE

The effective stress (σ_ϵ) used in Experiments II-1 to II-5 was determined to be 1-5 MPa based on the calculation of (1). The impact of effective stress on the permeability was examined by adjusting the axial and confining pressure and collecting the average flow rate of methane gas followed by the conversion to the gas permeability of coal sample (Figure 4).

The results indicate that the mechanism of the impact of effective stress on gas-containing coal can be simplified as the impact of axial and confining pressure on the coal body. The growth of effective stress increases both the axial and confining pressure, and enhances the compression of holes and cracks, which narrows the flow channel of methane gas. These effects together reduce the permeability of gas-containing coal. With the increase of axial and confining pressure, the compression effect on the holes and cracks inside the coal body becomes weaker,

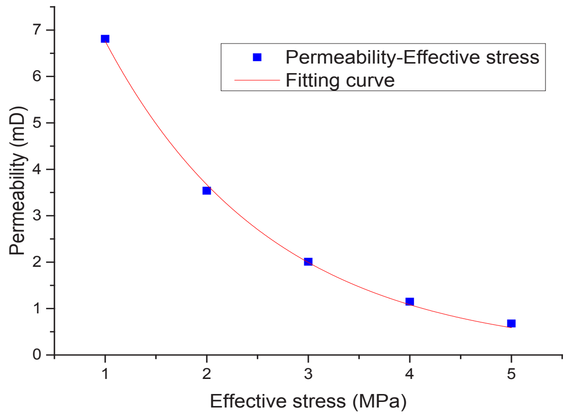

FIGURE 4. Permeability versus effective stress

slowing down the permeability change and eventually approximating a fixed value.

We also found that the impact of effective stress is smaller than that of confining pressure, but larger than axial pressure. This result is also in consistence with that from other researchers, in which an exponential relationship ($K=ae^{b\sigma_\epsilon}$) is used to correlate the permeability with effective stress (Zhang 2011):

$$K=ae^{b\sigma_\epsilon} , \tag{9}$$

where K is permeability (mD); σ_ϵ is effective stress (MPa); and a and b are constants.

Fitting permeability versus effective stress curve based on (6) gives:

$$K=12.45202e^{-0.6107\sigma_\varepsilon} , \tag{10}$$

The R^2 for this fit is 0.99823, showing good consistency between the fitted curve and experimental values. Therefore, for the #3 coal seam of JSRD Ltd., under the condition of effective stress σ_ϵ = 1-5 MPa, the permeability (K) of the coal sample can be regarded to follow the relationship described by Eq. 10. The measured effective stress of the coalbed can be used to provide a valuable basis for predicting gas permeability based on (10).

IMPACT OF GAS PRESSURE ON THE PERMEABILITY OF THE COAL SAMPLE

Experiment III focuses on the impact of gas pressure on the permeability of coal. In this study, constant temperature (T) was set at 25°C, negative pressure for draining (P_2) was set at -15 kPa, axial pressure (σ_1) was set at 4 MPa, confining pressure (σ_2) was set at 2, 4, 6 and 8 MPa. The gas permeability was obtained at gas pressure P_1 =0.5 and 1.5 MPa, respectively.

The experimental data (Figure 5) indicate that permeability of coal sample increases non-linearly with the increase of gas pressure, showing several clear stages.

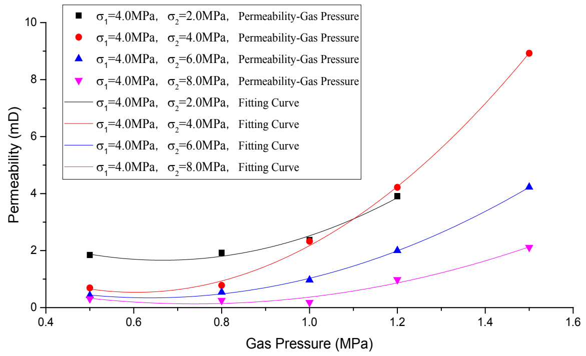

FIGURE 5. Fitted curve of permeability versus gas pressure

When axial and confining pressures are kept constant, permeability first decreases and then increases with the increase of gas pressure. Previous research has shown that there is a second-order polynomial relationship between permeability and gas pressure, i.e., there is a critical pressure in the permeability-gas pressure relationship. When gas pressure is greater than critical pressure, gas permeability decreases with the increase of gas pressure; however, when gas pressure is lower than critical pressure, gas permeability increases with gas pressure, showing a clear Klinkenberg effect. This study shows that under the conditions of axial pressure σ_1 =4.0 MPa and confining pressures of σ_2 =2, 4, 6, and 8 MPa, the Klinkenberg effect occurs in the range of gas pressure P_1<0.80 MPa. The result also shows that the critical pressure is different under different confining pressures. At confining pressure σ_2=2, 4, 6 and 8 MPa, the critical pressures of gas are P_ϕ = 0.65MPa, P_ϕ = 0.63MPa, P_ϕ = 0.72MPa, and P_ϕ = 0.80 MPa, respectively. Considering the Klinkenberg effect, the general relationship between gas pressure P_1 and permeability K is fitted and expressed as:

$$K=a+bP_1+cP_1, \tag{11}$$

where a, b and c are fitting coefficients.

Equation 11 was used to fit the experimental data from III-1 to III-4, and the fitted data are shown in Table 6.

TABLE 6. Fitted equation of permeability versus gas pressure based on experimental data

Group	Axial pressure (MPa)	Confining pressure (MPa)	Fitted equation	R^2
III-1	4	2	$K = 5.07385 - 10.24346p_1 + 7.68987p_1^2$	0.98731
III-2	4	4	$K = 4.36771 - 12.67014p_1 + 10.47611p_1^2$	0.99659
III-3	4	6	$K = 2.46367 - 6.65291p_1 + 5.21730p_1^2$	0.99153
III-4	4	8	$K = 2.00681 - 5.08161p_1 + 3.44340p_1^2$	0.99754

The goodness of fit in all four sets of data is high, indicating good consistency between the fitted curve and experimental data. However, except for III-1 in which confining pressure σ_2 = 2 MPa, the changing rate of permeability versus gas pressure decreases with the increase of confining pressure. Therefore, for the #3 coal seam of JSRD Ltd., under the condition of constant temperature, loaded stress, and negative pressure of draining, in the confining pressure range of σ_2 =2–8 MPa, the permeability (K) of the coal sample can be regarded to follow the relationship described by Table 6.

FIELD TEST

Based on the experimental results and the theoretical calculations for the coal samples, the impacts of axial pressure, confining pressure, gas pressure, and effective stress on permeability were obtained for 1301 fully mechanized coal faces in the JSRD Ltd. #3 coal seam. The permeability of the coal body is directly related to the natural flow rate of gas, concentration of gas drainage, and the damping coefficient. To verify the experimental study and theoretical calculation, we individually investigated the natural flow rate of gas, concentration of gas drainage, and damping coefficient by opening draining holes at Construction Zone #1 at 370 m burial depth (#15 coal seam) and Construction Zone #2 at 250 m burial depth (#3 coal seam), respectively.

TEST OF THE NATURAL FLOW RATE OF GAS AND DAMPING COEFFICIENT

The damping curve of gas flow rate versus time was fitted based on the measured flow rate data in the #1 and #2 draining holes (Figure 6). The damping coefficient α of flow rate at #1 draining hole is 0.077, which indicates the difficulty of gas draining. However, the damping

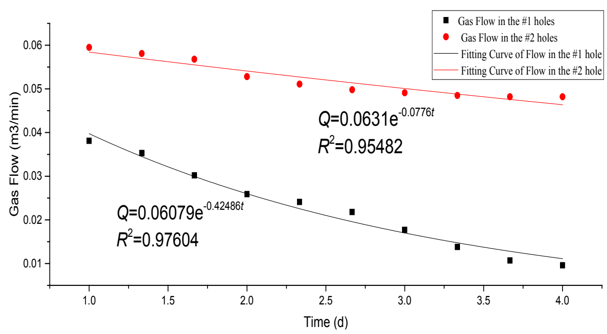

FIGURE 6. Natural flow rate of gas versus time for the #1 and #2 draining holes

coefficient α of flow rate at the #2 draining hole is 0.4713, reaching to a sufficient level that allows draining. This shows that the existence of ground stress largely affects the damping coefficient of the coal seam. Shallow regions have a smaller ground stress, thus possess a larger damping coefficient, whereas deep regions show the opposite effect.

Analysis of the results from field test

The #1 draining hole was opened at the burial depth of 370 m and the #2 draining hole was opened at the burial depth of 250 m. Based on Figure 6, the natural flow rate of gas from the #2 draining hole is much larger than that from the #1 draining hole. The damping coefficient of the #2 draining hole is larger than that of the #1 draining hole, indicating the large impact of ground stress on the natural flow rate of gas and the damping coefficient. This result is consistent with the aforementioned relationship between loaded stress and permeability. Compared with the #2 draining hole, the #1 draining hole has a lower single-hole draining rate, concentration of single-hole drainage concentration, daily amount of drainage, and monthly amount of drainage amount. This is also consistent with the aforementioned relationship between loaded stress and permeability.

By investigating the natural flow rate of gas, concentration of drainage and damping coefficient of draining holes at different burial depths, we have verified the relationship between loaded stress and gas permeability.

Conclusion

In this work, we systematically studied the impact of loaded stress on gas permeability of coal sample and the detailed experimental design and results were presented. The gas permeability was thoroughly analyzed in terms of axial pressure, confining pressure, effective stress, and gas pressure. Our major conclusions are as follows:

The increase of axial and confining pressure of coal sample increases the loaded effective stress of sample, causing compression of inner holes and cracks and thus the shrinkage of the gas flow channel. The original micro-porous structure is also damaged under external force, which causes plugging of the large holes and cracks in the coal body, thus reducing the gas permeability.

The impact of axial pressure on gas permeability is small. Axial pressure and permeability are correlated in a linear relationship. For the #3 coal seam of JSRD Ltd., under the conditions that the confining pressure is 2, 4, 6, 8 and 10MPa, and axial pressure is between 1 and 10 MPa, the permeability *K* of coal rock is believed to follow the following equations:,,,, and .

Confining pressure has a large impact on permeability. The relationship between confining pressure and permeability is exponential. For the #3 coal seam of JSRD Ltd., under the conditions that the confining pressure and axial pressure all lie between 1 and 10 MPa, the permeability *K* of coal rock can be regarded to follow the following equation: . Taking axial pressure into account, the relationship satisfies the following equation: .

Permeability and gas pressure are correlated in a second-order polynomial relationship because of the Klinkenberg effect. Permeability first decreases and then increases with the increase of gas pressure. At confining pressure = 2, 4, 6 and 8 MPa, the critical pressure of methane gas are = 0.65MPa, = 0.63MPa = 0.72MPa and =0.80 MPa, respectively. For the #3 coal seam of JSRD Ltd., under the condition of constant temperature, loaded stress, and negative pressure for draining, and in the confining pressure range of = 2-8 MPa, the permeability (*K*) of the coal sample can be regarded to follow the relationship described by Table 6.

Our investigation into the natural flow rate of gas, concentration of gas drainage and damping coefficient at draining holes of different burial depths supports the conclusion from the experimental study on the impact of loaded stress on gas permeability.

Acknowledgements

We thank LetPub (www.letpub.com) for its linguistic assistance during the preparation of this paper. This research did not receive any specific grant from funding agencies in the public, commercial or not-for-profit sectors. The authors declare that there is no conflict of interest.

References

Bobo L. 2014. Study on the mechanism of coal damage evolution and coal seam gas permeation under different the mining conditions. Thesis. Chongqing University (unpublished).

Fathi, E. & Akkutlu, I.Y. 2009. Matrix heterogeneity effect on gas transport and adsorption in coalbed and shale gas reservoirs. *Transport in Porous Media* 80(2): 281-304.

Fedorov, A.V. & Fedorchenko, I.A. 2009. Mathematical modeling of methane flow in coal beds. *Journal of Mining Science* 45(1): 9-21.

Han, F. & Busch, A. 2009. Experimental study of gas and water transport processes in the inter-cleat (*matrix)* system of coal: *Anthracite* from Qinshui Basin, China. *International Journal of Coal Geology* 81(2): 128-138.

Kadir, R.A., Siddiq, A.N.A., Yahya, N.A., Rusdi, A.R., Hazli, Z. & Hussain, H. 2013. Audience response system (ARS) technology and dentist attendance in smoking cessation workshop. *Sains Malaysiana* 42(1): 1-5.

Kamsani, S.R., Ibrahim, N. & Ishak, N.A. 2017. Psychological debriefing intervention: From the lens of disaster volunteers. *Malaysian Journal of Geoscience* 1(1): 32-33.

Kunyun, T. 2014. Research on the deformation characteristics and gas seepage rule of coal body loaded by high pressure water. Thesis. China University of Mining and Technology Beijing (unpublished).

Lai, G.T., Razib, A.M.M., Mazlan, N.A., Rafek, A.G., Serasa, A.S., Simon, N., Surip, N., Ern, L.K., Rusli, T. & Mohamed. 2017. Rock slope stability assessment of limestone hills in Northern Kinta Valley, Ipoh, Perak, Malaysia. *Geological Behavior* 1(1): 16-18.

Mavor, M.J. & Gunter, W.D. 2006. Secondary porosity and permeability of coal vs. gas composition and pressure. *SPE Reservoir Evaluation & Engineering* 9(2): 114-125.

Mingyao, W. 2013. Study of gas-solid coupling seepage flow in coal containing methane and its application. Thesis. China University of Mining and Technology (unpublished).

Palmer, I. 2008. Permeability changes in coal: Analytical modeling. *International Journal of Coal Geology* 77(1): 119-126.

Pan, Z. & Connell, L.D. 2010. Laboratory characterisation of coal reservoir permeability for primary and enhanced coalbed methane recovery. *International Journal of Coal Geology* 82(3-4): 252-261.

Peng, Y.W., Qi, Q.X., Deng, Z.G. & Li, H.Y. 2008. Experimental research on sensibility of permeability of coal samples under confining pressure status based on scale effect. *Journal of China Coal Society* 33(5): 509-513.

Sun, P. & Ling, Z. 2000. Experimental study of the law for permeability of coal under action of 3-triaxial compression. *Journal of Chongqing University* (Natural Science Edition) (S1) 28-31.

Wang, G.R., Xue, D.J., Gao, H.L. & Zhou, H.W. 2012. Study on permeability characteristics of coal rock in complete stress-strain process. *Journal of China Coal Society* 37(1): 107-112.

Wang, G.X., Massarotto, P. & Rudolph, V. 2008. An improved permeability model of coal for coalbed methane recovery and CO_2 geosequestration. *International Journal of Coal Geology* 77(1): 127-136.

Yi, J., Jiang, Y. & Xian, X. 2007. An experimental research on the characters of methane seepage in stress field and temperature field. *China Mining Magazine* 2007-05.

Zhang, D. 2011. Experimental study on mechanical characteristics and seepage characteristics of coal containing methane under the coupling effect between stress and thermal. Thesis. Chongqing University, Chongqing (unpublished).

Dengxing Qu
School of Civil Engineering and Architecture
Wuhan University of Technology
Wuhan, Hubei 430070
China

Xinping Li
Hubei Key Laboratory of Roadway Bridge and Structure Engineering
Wuhan University of Technology
Wuhan Hubei 430070
China

Jianhua Zhang*, Dengke Li
School of Resources and Environmental Engineering
Wuhan University of Technology
Wuhan 430070
China

Gongzhong Wang
Department of Safety Science & Engineering
Henan Institute of Engineering
Zhengzhou 451191
China

*Corresponding author; email: zjhwut@sina.com

Received: 5 January 2017
Accepted: 20 May 2017